AIAA JOURNAL
Vol. 43, No. 6, June 2005

Thermal Postbuckling Characteristics of Laminated Conical Shells with Temperature-Dependent Material Properties

B. P. Patel*
Institute of Armament Technology, Pune 411 025, India
K. K. Shukla†
Motilal Nehru National Institute of Technology, Allahabad 211 004, India
and
Y. Nath‡
Indian Institute of Technology Delhi, New Delhi 110 016, India

The nonlinear thermoelastic buckling/postbuckling characteristics of laminated circular conical/cylindrical shells subjected to uniform temperature rise are studied employing semi-analytical finite element approach based on first-order shear deformation theory and field consistency principle. The nonlinear governing equations, considering geometric nonlinearity based on von Kármán's assumption for moderately large deformation, are solved using Newton–Raphson iteration procedure coupled with displacement control method to trace the prebuckling/postbuckling equilibrium path. The presence of asymmetric perturbation in the form of small magnitude load spatially proportional to the linear buckling mode shape is assumed to initiate the bifurcation of the shell deformation. The study is carried out to highlight the influences of semicone angle, number of layers, material properties, and number of circumferential waves on the nonlinear thermoelastic response of the laminated circular conical/cylindrical shells. The participation of axisymmetric and asymmetric modes in the total response of the shells is brought out through the deformation shape analysis. The comparison of thermoelastic pre- and postbuckling characteristics of shells with temperature-dependent material properties is made with those considering constant material properties, and the behavior is found to be significantly different depending upon the shell parameters and degradation rate of material properties. The shells exhibit softening type of prebuckling nonlinear response and snap-through-type/stable postbuckling response depending upon the geometrical/material parameters.

I. Introduction

THE modern aeronautical and other engineering structures, such as supersonic and hypersonic aircraft, rockets, satellites, as well as electronic equipment, nuclear components, etc., are often expected to operate at elevated temperatures. The advances in composite technology have led to the application of elevated-temperature composite structural elements, such as cylindrical and conical shells, tailored for the required performance as load-bearing members in the design of more and more sophisticated futuristic structures. Also, the conical shells are often used as transition elements between cylinders of different diameter and/or end closures in various engineering applications such as tanks and pressure vessels, missiles and spacecraft, submarines, etc. The temperature rise in these structural elements caused by boundary restraints can introduce compressive membrane state of stress leading to thermoelastic instabilities/buckling failures. An estimate of the critical buckling temperature can be made through a linear eigenvalue analysis, whereas the sensitivity to the imperfections and postbuckling behavior is evaluated by means of nonlinear analysis. For the later analyses, generally in the literature, an imperfection/perturbation affine to the critical buckling mode evaluated from eigenvalue analysis is assumed to be present in the shell structures.

The thermal buckling studies of composite laminated shells have received limited attention in the literature compared to those of isotropic shells and laminated panels.[1–3] The available literature on laminated shells is mostly dealing with the thermoelastic buckling characteristics of circular cylindrical shells.[4–17] The critical buckling temperatures of laminated composite cylindrical shells are estimated based on linear eigenvalue approach by using Semiloof shell finite element,[4,5] employing Galerkin method for approximate analytical solution of improved Donnell's equations,[6] and semi-analytical finite element based on first-order shear deformation theory.[7,8] The buckling and postbuckling response of composite shells subjected to high temperature is studied by Birman and Bert[9] employing nonlinear thermoelastic version of Love's first approximation theory and snap-through type of behavior is discussed qualitatively. The postbuckling analyses of perfect and imperfect, unstiffened and stiffened, multilayered cross-ply cylindrical shells under thermomechanical loading situations have been performed by using von Kármán–Donnell theory and employing singular perturbation approach.[10–14] The dynamic effects on the stability characteristics of laminated cylindrical shells arising as a result of the sudden application of the thermal load[15,16] and the presence of periodic time-dependent temperature filed[17] are also investigated in the literature.

The studies on the thermoelastic buckling characteristics of conical shells are mostly dealing with the isotropic shells,[18–22] except the work of Wu and Chiu.[23,24] This can be attributed to the inherent complexity of the basic equations in curvilinear circular conical coordinates, which are a system of nonlinear partial differential equations with variable coefficients. Thermoelastic buckling[23] and thermally induced dynamic instability[24] of laminated composite conical shells are investigated employing perturbation approach to solve the linear three-dimensional equations of motion. The initial prebuckling thermal stresses are evaluated directly by multiplying thermal strains with the constitutive matrix.[23,24] However, it has been brought out in the literature that the prebuckling state of stress has to be determined using the deformation filed obtained from the static analysis of the shells subjected to assumed temperature distribution.

In all of the studies just cited,[4–24] the elastic and thermal properties of materials are considered to be independent of temperature.

Received 6 September 2004; revision received 26 November 2004; accepted for publication 7 January 2005.

*Scientist, Mechanical Engineering Faculty, Girinagar; currently Assistant Professor, Department of Applied Mechanics, Indian Institute of Technology Delhi, New Delhi 110 016, India.
†Reader, Department of Applied Mechanics.
‡Professor, Department of Applied Mechanics.

However, the material properties are known to degrade with the rise of temperature[25]; therefore, it is more appropriate to take into account the temperature-dependent material properties for accurate/rigorous design/analysis. Thermal postbuckling analysis of laminated plates[26–29] and curved panels,[30] and thermal buckling of local delamination[31] near the surface of laminated cylindrical shell are studied considering temperature-dependent material properties.

To optimally exploit the strength and load-carrying capacity of laminated composite conical/cylindrical shells at elevated temperatures, accurate prediction and understanding of their thermal buckling/postbuckling characteristics considering temperature-dependent material properties is important. However, to the authors' knowledge, the study on the thermoelastic buckling/postbuckling behavior of laminated conical/cylindrical shells with temperature-dependent material properties appears to be scarce in the literature. The participation of axisymmetric/asymmetric modes is also not brought out clearly in the limited number of analytical investigations available on thermal postbuckling behavior of cylindrical shells.

Therefore, in the present work the thermoelastic buckling/postbuckling characteristics of laminated truncated circular conical/cylindrical shells subjected to uniform temperature rise are studied through nonlinear static analysis employing semi-analytical finite element approach. Geometric nonlinearity is introduced in the formulation by using von Kármán's strain-displacement relations. The presence of asymmetric perturbation in the form of small-magnitude load spatially proportional to the linear buckling mode shape is assumed to initiate the bifurcation of the shell deformation from axisymmetric mode to asymmetric one. The study is carried out to highlight the influences of semicone angle, number of layers, material properties, and number of circumferential waves on the nonlinear thermoelastic response of the laminated circular conical/cylindrical shells. The comparison of thermoelastic postbuckling characteristics of shells with temperature-dependent material properties is made with those considering constant material properties, and the behavior is found to be significantly different depending upon the shell parameters and degradation rate of material properties. The participation of axisymmetric and asymmetric modes in the total response of the shells is also highlighted through the deformation shape analysis.

II. Formulation

An axisymmetric laminated composite shell of revolution is considered with the coordinates s, θ, and z along the meridional, circumferential, and radial/thickness directions, respectively. The displacements u, v, w at a point (s, θ, z) from the median surface are expressed as functions of middle-surface displacements u_0, v_0, and w_0, and independent rotations β_s and β_θ of the meridional and hoop sections, respectively, as

$$\begin{aligned} u(s,\theta,z) &= u_0(s,\theta) + z\,\beta_s(s,\theta) \\ v(s,\theta,z) &= v_0(s,\theta) + z\,\beta_\theta(s,\theta) \\ w(s,\theta,z) &= w_0(s,\theta) \end{aligned} \tag{1}$$

Using the semi-analytical approach, u_0, v_0, w_0, β_s, and β_θ are represented by a Fourier series in the circumferential angle θ. For the nth harmonic, these can be written as[32]

$$\begin{aligned} u_0(s,\theta) &= u_0^0(s) + \sum_{i=1}^{4}\left[u_0^{c_i}(s)\cos(in\theta) + u_0^{s_i}(s)\sin(in\theta)\right] \\ v_0(s,\theta) &= v_0^0(s) + \sum_{i=1}^{4}\left[v_0^{c_i}(s)\cos(in\theta) + v_0^{s_i}(s)\sin(in\theta)\right] \\ w_0(s,\theta) &= w_0^0(s) + \sum_{i=1}^{2}\left[w_0^{c_i}(s)\cos(in\theta) + w_0^{s_i}(s)\sin(in\theta)\right] \\ \beta_s(s,\theta) &= \beta_s^0(s) + \sum_{i=1}^{2}\left[\beta_s^{c_i}(s)\cos(in\theta) + \beta_s^{s_i}(s)\sin(in\theta)\right] \\ \beta_\theta(s,\theta) &= \beta_\theta^0(s) + \sum_{i=1}^{2}\left[\beta_\theta^{c_i}(s)\cos(in\theta) + \beta_\theta^{s_i}(s)\sin(in\theta)\right] \end{aligned} \tag{2}$$

where superscript 0 refers to the axisymmetric component of displacement field variables, and c_i and s_i refer to the asymmetric components of the field variables having circumferential variation proportional to $\cos(in\theta)$ and $\sin(in\theta)$, respectively.

The preceding displacement variations in the circumferential direction are chosen according to the physics of the large deformation of shells of revolution, that is, participation of axisymmetric mode and higher asymmetric modes.[32–36] Additional terms in the in-plane displacements, compared to radial displacement, are added to keep the nonlinear membrane strains consistent.

With von Kármán's assumption for moderately large deformation, Green's strains can be written in terms of midsurface deformations as

$$\{\varepsilon\} = \begin{Bmatrix} \varepsilon_p^L \\ 0 \end{Bmatrix} + \begin{Bmatrix} z\varepsilon_b \\ \varepsilon_s \end{Bmatrix} + \begin{Bmatrix} \varepsilon_p^{NL} \\ 0 \end{Bmatrix} \tag{3}$$

where the membrane strains $\{\varepsilon_p^L\}$, bending strains $\{\varepsilon_b\}$, shear strains $\{\varepsilon_s\}$, and nonlinear in-plane strains $\{\varepsilon_p^{NL}\}$ in Eq. (3) are written as[37]

$$\left\{\varepsilon_p^L\right\} = \begin{Bmatrix} \dfrac{\partial u_0}{\partial s} + \dfrac{w_0}{R} \\ \dfrac{u_0\sin\phi}{r} + \dfrac{\partial v_0}{r\partial\theta} + \dfrac{w_0\cos\phi}{r} \\ \dfrac{\partial u_0}{r\partial\theta} - \dfrac{v_0\sin\phi}{r} + \dfrac{\partial v_0}{\partial s} \end{Bmatrix}$$

$$\{\varepsilon_b\} = \begin{Bmatrix} \dfrac{\partial\beta_s}{\partial s} + \dfrac{\partial u_0}{R\partial s} \\ \dfrac{\beta_s\sin\phi}{r} + \dfrac{\partial\beta_\theta}{r\partial\theta} + \dfrac{u_0\sin\phi}{Rr} \\ \dfrac{1}{R}\dfrac{\partial u_0}{r\partial\theta} + \dfrac{\partial v_0}{\partial s}\dfrac{\cos\phi}{r} + \dfrac{\partial\beta_s}{r\partial\theta} + \dfrac{\partial\beta_\theta}{\partial s} - \dfrac{\beta_\theta\sin\phi}{r} \end{Bmatrix}$$

$$\{\varepsilon_s\} = \begin{Bmatrix} \beta_s + \dfrac{\partial w_0}{\partial s} \\ \beta_\theta + \dfrac{\partial w_0}{r\partial\theta} - \dfrac{v_0\cos\phi}{r} \end{Bmatrix}, \qquad \left\{\varepsilon_p^{NL}\right\} = \begin{Bmatrix} \dfrac{1}{2}\left(\dfrac{\partial w_0}{\partial s}\right)^2 \\ \dfrac{1}{2}\left(\dfrac{\partial w_0}{r\partial\theta}\right)^2 \\ \dfrac{\partial w_0}{\partial s}\dfrac{\partial w_0}{r\partial\theta} \end{Bmatrix} \tag{4}$$

where r, R, and ϕ are the radius of the parallel circle, radius of the meridional circle, and angle made by the tangent at any point in the shell with the axis of revolution.

If $\{\boldsymbol{N}\}$ represents the stress resultants $(N_{ss}, N_{\theta\theta}, N_{s\theta})$ and $\{\boldsymbol{M}\}$ the moment resultants $(M_{ss}, M_{\theta\theta}, M_{s\theta})$, one can relate these to membrane strains $\{\varepsilon_p\}$ $(=\{\varepsilon_0^L\}+\{\varepsilon_0^{NL}\})$ and bending strains $\{\varepsilon_b\}$ through the constitutive relations as

$$\begin{Bmatrix} \{\boldsymbol{N}\} \\ \{\boldsymbol{M}\} \end{Bmatrix} = \begin{bmatrix} [\boldsymbol{A}] & [\boldsymbol{B}] \\ [\boldsymbol{B}] & [\boldsymbol{D}] \end{bmatrix} \begin{Bmatrix} \{\varepsilon_p\} \\ \{\varepsilon_b\} \end{Bmatrix} - \begin{Bmatrix} \{\bar{\boldsymbol{N}}\} \\ \{\bar{\boldsymbol{M}}\} \end{Bmatrix} \tag{5}$$

where $[\boldsymbol{A}]$, $[\boldsymbol{D}]$, and $[\boldsymbol{B}]$ are extensional, bending, and bending-extensional coupling stiffness coefficients matrices of the composite laminate. $\{\bar{\boldsymbol{N}}\}$ and $\{\bar{\boldsymbol{M}}\}$ are the thermal stress and moment resultants, respectively.

Similarly, the transverse shear force $\{\boldsymbol{Q}\}$ representing the quantities $(Q_{sz}, Q_{\theta z},)$ are related to the transverse shear strains $\{\varepsilon_s\}$ through the constitutive relation as

$$\{\boldsymbol{Q}\} = [\boldsymbol{E}]\{\varepsilon_s\} \tag{6}$$

where $[\boldsymbol{E}]$ is the transverse shear stiffness coefficients matrix of the laminate.

For a laminated shell of thickness h, consisting of N layers with stacking angles $\theta_i (i = 1, \ldots, N)$ and layer thicknesses

$h_i (i = 1, \ldots, N)$, the necessary expressions to compute the stiffness coefficients and thermal stress/moment resultants, available in the literature[38] are used here.

The potential energy functional $U_1(\boldsymbol{\delta})$ (as a result of strain energy and transverse load) is given by

$$U_1(\boldsymbol{\delta}) = \frac{1}{2}\int_A \left[\begin{Bmatrix} \varepsilon_p \\ \varepsilon_b \end{Bmatrix}^T \begin{bmatrix} \boldsymbol{A} & \boldsymbol{B} \\ \boldsymbol{B} & \boldsymbol{D} \end{bmatrix} \begin{Bmatrix} \varepsilon_p \\ \varepsilon_b \end{Bmatrix} + \{\varepsilon_s\}^T [\boldsymbol{E}] \{\varepsilon_s\} - \begin{Bmatrix} \varepsilon_p \\ \varepsilon_b \end{Bmatrix}^T \begin{Bmatrix} \bar{\boldsymbol{N}} \\ \bar{\boldsymbol{M}} \end{Bmatrix} \right] \mathrm{d}\boldsymbol{A} - \int_A \boldsymbol{q}\, w_0 \, \mathrm{d}\boldsymbol{A} \tag{7}$$

where $\boldsymbol{\delta}$ is the vector of degrees of freedom associated to the displacement field in a finite element discretization and q is the applied external pressure load.

The potential energy $U_2(\boldsymbol{\delta})$ due to initial state of in-plane stress resultants $\{\boldsymbol{N}^0\} = \{N^0_{ss} \;\; N^0_{\theta\theta} \;\; N^0_{s\theta}\}^T$ is written as

$$U_2(\boldsymbol{\delta}) = \int_A \{\varepsilon_{\mathrm{NL}}\}^T \{\boldsymbol{N}^0\} \, \mathrm{d}A \tag{8}$$

Following the procedure given in the work of Rajasekaran and Murray,[39] the total potential energy functional $U(\boldsymbol{\delta})\,[= U_1(\boldsymbol{\delta}) + U_2(\boldsymbol{\delta})]$ can be expressed as

$$U(\boldsymbol{\delta}) = \{\boldsymbol{\delta}\}^T \big[(1/2)[[\boldsymbol{K}] - [\boldsymbol{K}_T] + [\boldsymbol{K}_G]] + (1/6)[\boldsymbol{N}_1(\boldsymbol{\delta})] + (1/12)[\boldsymbol{N}_2(\boldsymbol{\delta})] \big] \{\boldsymbol{\delta}\} - \{\boldsymbol{\delta}\}^T \{\boldsymbol{F}_M\} - \{\boldsymbol{\delta}\}^T \{\boldsymbol{F}_T\} \tag{9}$$

where $[\boldsymbol{K}]$ is the linear stiffness matrix and $[\boldsymbol{N}_1]$ and $[\boldsymbol{N}_2]$ are nonlinear stiffness matrices linearly and quadratically dependent on the field variables, respectively. $[\boldsymbol{K}_T]$ and $[\boldsymbol{K}_G]$ are the geometric stiffness matrices due to thermal and initial stress resultants. $\{\boldsymbol{F}_M\}$ and $\{\boldsymbol{F}_T\}$ are mechanical and thermal load vectors.

The minimization of total potential $U(\boldsymbol{\delta})$ given in Eq. (9) with respect to vector of degrees of freedom $\boldsymbol{\delta}$ leads to the governing equation for the deformation of the shell as

$$\big[[\boldsymbol{K}] - [\boldsymbol{K}_T] + [\boldsymbol{K}_G] + \left(\tfrac{1}{2}\right)[\boldsymbol{N}_1(\boldsymbol{\delta})] + \left(\tfrac{1}{3}\right)[\boldsymbol{N}_2(\boldsymbol{\delta})] \big] \{\boldsymbol{\delta}\} = \{\boldsymbol{F}_M\} + \{\boldsymbol{F}_T\} \tag{10}$$

The governing Eq. (10) can be employed to study the linear/nonlinear static and eigenvalue buckling analyses by neglecting the appropriate terms as follows.

Linear static analysis:

$$[\boldsymbol{K}]\{\boldsymbol{\delta}\} = \{\boldsymbol{F}_M\} + \{\boldsymbol{F}_T\} \tag{11}$$

Nonlinear static analysis:

$$\big[[\boldsymbol{K}] - [\boldsymbol{K}_T] + \left(\tfrac{1}{2}\right)[\boldsymbol{N}_1(\boldsymbol{\delta})] + \left(\tfrac{1}{3}\right)[\boldsymbol{N}_2(\boldsymbol{\delta})] \big] \{\boldsymbol{\delta}\} = \{\boldsymbol{F}_M\} + \{\boldsymbol{F}_T\} \tag{12}$$

Eigenvalue buckling analysis:

$$[\boldsymbol{K}]\{\boldsymbol{\delta}\} = \Delta T \big[\boldsymbol{K}^*_G\big] \{\boldsymbol{\delta}\} \tag{13}$$

where $[\boldsymbol{K}^*_G]$ is the geometric stiffness caused by initial state of stress developed because of unit uniform temperature rise and ΔT is the temperature rise.

For the purpose of evaluating $[\boldsymbol{K}^*_G]$, first the static analysis of the shell using Eq. (11) for unit temperature rise is carried out. The resulting deformation field is used to calculate the initial state of stress resultants using Eq. (5) and, in turn, for evaluating the $[\boldsymbol{K}^*_G]$ matrix.

The nonlinear prebuckling followed by postbuckling equilibrium path is traced by solving Eq. (12) using a Newton–Raphson iteration procedure coupled with displacement control method.[40] The degree of freedom for which the increment in the last step is the highest is selected as a control parameter. The equilibrium iterations are continued for each load/displacement step until the convergence criteria suggested by Bergan and Clough[41] are satisfied within the specific tolerance limit of less than 0.001%.

III. Element Description

The laminated axisymmetric shell element used here is a C^0 continuous shear flexible element and has 33 nodal degrees of freedom

$$u^0_0, u^{c1}_0, u^{s1}_0, u^{c2}_0, u^{s2}_0, u^{c3}_0, u^{s3}_0, u^{c4}_0, u^{s4}_0, v^0_0, v^{c1}_0, v^{s1}_0,$$
$$v^{c2}_0, v^{s2}_0, v^{c3}_0, v^{s3}_0, v^{c4}_0, v^{s4}_0, w^0_0, w^{c1}_0, w^{s1}_0, w^{c2}_0,$$
$$w^{s2}_0, \beta^0_s, \beta^{c1}_s, \beta^{s1}_s, \beta^{c2}_s, \beta^{s2}_s, \beta^0_\theta, \beta^{c1}_\theta, \beta^{s1}_\theta, \beta^{c2}_\theta, \beta^{s2}_\theta$$

at three nodes in a curved element leading to 99 degrees of freedom per element.

If the interpolation functions for three-noded element are used directly to interpolate the five field variables u_0, v_0, w_0, β_s, and β_θ in deriving the transverse shear and membrane strains, the element will lock and show oscillations in the shear and membrane stresses. Field consistency requires that the membrane and transverse shear strains must be interpolated in a consistent manner. Thus, β_s term in the expression for $\{\varepsilon_s\}$ given in Eq. (4) has to be consistent with field function $\partial w_0/\partial s$ as shown in the works of Balakrishna and Sarma[42] and Prathap and Ramesh Babu.[43] Similarly the w_0 and (u_0, v_0) terms in the expression of $\{\varepsilon^L_p\}$ (first and third strain components) have to be consistent with the field functions $\partial u_0/\partial s$ and $\partial v_0/\partial s$, respectively. This is achieved by using the field redistributed substitute shape functions to interpolate those specific terms that must be consistent as described by Prathap and Ramesh Babu.[43] The element derived in this fashion behaves very well for both thick and thin situations and permits the greater flexibility in the choice of integration order for the energy terms. Because the element is based on the field consistency approach, all of the strain-energy terms are evaluated using an exact numerical integration scheme with respect to the meridional coordinate s. The integration in the circumferential direction is carried out explicitly. The element employed here has good convergence and has no spurious rigid modes.

IV. Results and Discussion

Here, the thermoelastic nonlinear prebuckling path followed by postbuckling characteristics of laminated truncated circular conical shells $(1/R = 0)$ subjected to uniform temperature rise are investigated using the semi-analytical finite element formulation. The radius of the parallel circle of the conical shell is expressed as $r = r_1 + (r_2 - r_1)\, s/L$, where r_1 and r_2 are the radii at the small and large end of the conical shell and L is the slant length. The parametric study is carried out to highlight the influences of semicone angle ϕ, number of layers N, material properties, and number of circumferential waves n on the nonlinear prebuckling/postbuckling response described as relationship between maximum outward normal displacement parameter $w_{\max}/h$ vs temperature rise ΔT for the laminated circular conical/cylindrical shells. The comparison of thermoelastic response of shells considering thermal degradation of material properties is made with that of considering temperature-independent (TID) properties.

The material properties used for the detailed studies are given next.

Material 1

The variation of the mechanical properties and coefficients of thermal expansion with temperature[27,28,30,44] is given in Table 1. In Table 1, E, G, ν, and α are Young's modulus, shear modulus, Poisson's ratio, and coefficient of thermal expansion, respectively. The subscripts L and T are the longitudinal and transverse directions

Table 1 Temperature-dependent properties of material 1 ($G_{TT} = G_{LT}$, $\nu_{LT} = \nu_{TT} = 0.28$)

	Temperature, °C			
Property	20	200	260	600
E_L, GPa	141	141	141	141
E_T, GPa	13.1	10.3	0.138	0.0069
G_{LT}, GPa	9.31	7.45	0.069	0.0034
α_T, $10^{-6}/°C$	0.018	0.054	0.054	0.054
α_L, $10^{-6}/°C$	21.6	37.8	37.8	37.8

respectively with respect to the fibers. These properties are evaluated in the work of Chen et al.[44] based on the rule of mixtures in conjunction with a glass transition temperature of 200°C for epoxy, retention of graphite fiber stiffness till 3000°C, and limited experiments. Between any of the two specified temperatures, the material properties are assumed to degrade linearly. The reference temperature is taken as 20°C.

Material 2

The temperature-dependent elastic constants and coefficients of thermal expansion are assumed to be linear functions of temperature change ΔT and are expressed as[31]

$$E_L(T) = E_L^0\left(1 - E_L^1\Delta T\right), \qquad E_T(T) = E_T^0\left(1 - E_T^1\Delta T\right)$$

$$G_{\mathrm{LT}}(T) = G_{\mathrm{LT}}^0\left(1 - G_{\mathrm{LT}}^1\Delta T\right), \qquad G_{\mathrm{TT}}(T) = G_{\mathrm{TT}}^0\left(1 - G_{\mathrm{TT}}^1\Delta T\right)$$

$$\alpha_L(T) = \alpha_L^0\left(1 + \alpha_L^1\Delta T\right), \quad \alpha_T(T) = \alpha_T^0\left(1 + \alpha_T^1\Delta T\right) \quad (14a)$$

where

$$E_L^0 = 181\,\mathrm{GPa}, \quad E_T^0 = 10.3\,\mathrm{GPa}, \quad G_{\mathrm{LT}}^0 = G_{\mathrm{TT}}^0 = 7.17\,\mathrm{GPa}$$

$$\nu_{\mathrm{LT}} = \nu_{\mathrm{TT}} = 0.28, \qquad \alpha_L^0 = 0.02 \times 10^{-6}/^\circ\mathrm{C}$$

$$\alpha_T^0 = 22.5 \times 10^{-6}/^\circ\mathrm{C}, \quad E_L^1 = E_T^1 = G_{\mathrm{LT}}^1 = G_{\mathrm{TT}}^1 = 0.5 \times 10^{-3}$$

$$\alpha_L^1 = \alpha_T^1 = 0.2 \times 10^{-3} \quad (14b)$$

Here, the superscripts 0 and 1 refer to the values at reference temperature and constant coefficients, respectively.

Material 3

The material property variation with temperature rise is assumed similar to material 2. The different material constants are taken as[26,29]

$$E_L^0 = 208\,\mathrm{GPa}, \quad E_T^0 = 5.2\,\mathrm{GPa}, \quad G_{\mathrm{LT}}^0 = 2.6\,\mathrm{GPa}$$

$$G_{\mathrm{TT}}^0 = 1.04\,\mathrm{GPa}, \quad \nu_{\mathrm{LT}} = \nu_{\mathrm{TT}} = 0.25, \quad \alpha_L^0 = \alpha_T^0 = 1 \times 10^{-6}/^\circ\mathrm{C}$$

$$E_L^1 = 0.5 \times 10^{-3}, \quad E_T^1 = G_{\mathrm{LT}}^1 = G_{\mathrm{TT}}^1 = 0.2 \times 10^{-3}$$

$$\alpha_L^1 = \alpha_T^1 = 0.5 \times 10^{-3} \quad (15)$$

The properties at reference temperature ($\Delta T = 0$) are used in the analysis for the TID material property assumption case. All of the layers are of equal thickness, and the ply angle is measured with respect to the meridional axis (s axis). The first layer is the innermost layer of the shell.

The details of simply supported and clamped–clamped immovable boundary conditions considered here at the two ends ($s = 0, L$) of the shell are as follows.

Simply supported:

$$u_0^0 = u_0^{c1} = u_0^{s1} = u_0^{c2} = u_0^{s2} = u_0^{c3} = u_0^{s3} = u_0^{c4} = u_0^{s4} = v_0^0 = v_0^{c1} = v_0^{s1}$$
$$= v_0^{c2} = v_0^{s2} = v_0^{c3} = v_0^{s3} = v_0^{c4} = v_0^{s4} = 0$$

$$w_0^0 = w_0^{c1} = w_0^{s1} = w_0^{c2} = w_0^{s2} = \beta_\theta^0 = \beta_\theta^{c1} = \beta_\theta^{s1} = \beta_\theta^{c2} = \beta_\theta^{s2} = 0 \quad (16)$$

Clamped–clamped:

$$u_0^0 = u_0^{c1} = u_0^{s1} = u_0^{c2} = u_0^{s2} = u_0^{c3} = u_0^{s3} = u_0^{c4} = u_0^{s4} = v_0^0 = v_0^{c1} = v_0^{s1}$$
$$= v_0^{c2} = v_0^{s2} = v_0^{c3} = v_0^{s3} = v_0^{c4} = v_0^{s4} = 0$$

$$w_0^0 = w_0^{c1} = w_0^{s1} = w_0^{c2} = w_0^{s2} = \beta_s^0 = \beta_s^{c1} = \beta_s^{s1} = \beta_s^{c2} = \beta_s^{s2} = \beta_\theta^0$$
$$= \beta_\theta^{c1} = \beta_\theta^{s1} = \beta_\theta^{c2} = \beta_\theta^{s2} = 0 \quad (17)$$

Based on progressive mesh refinement, 48 elements idealization is found to be adequate to model the complete slant length of the conical shells. Before proceeding for the detailed studies, the comparison of thermal postbuckling behavior predicted based on the present formulation is made with the work of Shen[11] for cross-ply laminated cylindrical shells. The results are presented in Fig. 1 as temperature parameter $\lambda_T (=10^3\alpha_0\Delta T)$ vs maximum inward asymmetric displacement (w_0^{c1}/h) curve and are found to be in good agreement. The present formulation is also validated by comparing the critical bifurcation temperature value of 96.6578°F (53.6988°C), evaluated from the present nonlinear analysis for a clamped-clamped conical shell fabricated from brass sheet ($r_1/h = 366$, $L/r_1 = 2.83$, $h = 0.005$ in., $\alpha = 10.4 \times 10^{-6}/^\circ\mathrm{F}$, $\phi = 15$ deg) with the theoretical result of 98°F (54.4444°C) reported in the work of Chang and Lu.[20] However, the experimental value of buckling temperature observed by Chang and Lu[20] is 128°F (71.1111°C). The discrepancy between the theoretical and experimental results is attributed to the determination of buckling by visual inspection.[20] To clarify this, the nonlinear thermoelastic response of the shell evaluated in the present study is depicted in Fig. 2. It can be observed that the shell shows a snap-through type of postbuckling response and the maximum outward displacement at 128°F temperature is about three times the thickness of the shell, whereas the inward displacement (not shown in the figure) is about six times of the thickness. For the thin shell considered in experimental investigation,[20] this amplitude level of deformation can be considered being visually observable.

Next, the nonlinear thermoelastic response characteristics of two- and eight-layered cross-ply laminated simply supported conical shells ($L/r_1 = 1$, $r_1/h = 500$, material 1) are shown in Fig. 3 for different values of semicone angle ($\phi = 0$, 30, and 60 deg) considering TID and temperature-dependent material properties. The

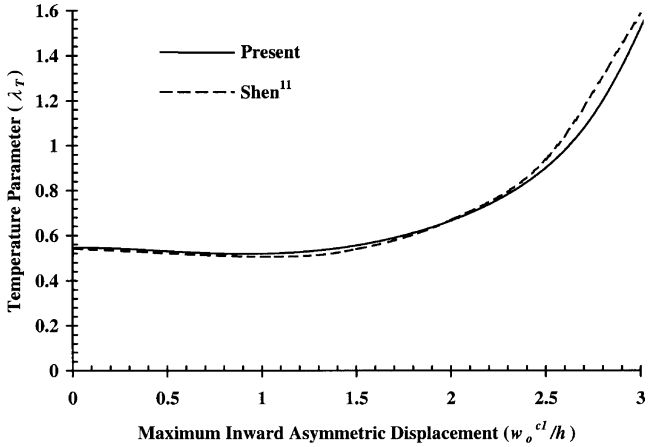

Fig. 1 Comparision of thermal postbuckling curve for cross-ply $(0/90\ \mathrm{deg})_S$ laminated clamped–clamped cylindrical shell ($L = 3$ m, $r_1 = r_2 = 3.8197$ m, $h = 0.01$ m; $E_L = 130.3$ GPa, $E_T = 9.377$ GPa, $G_{\mathrm{LT}} = 4.502$ GPa, $\nu_{\mathrm{LT}} = 0.33$, $\alpha_L = 0.139 \times 10^{-6}$, $\alpha_T = 9.0 \times 10^{-6}$, $n = 14$).

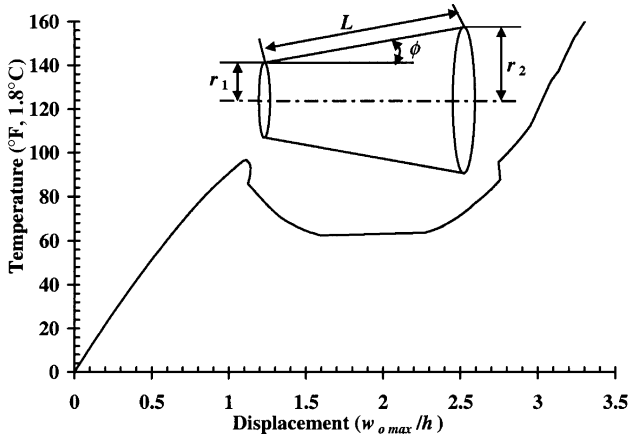

Fig. 2 Temperature vs maximum displacement curve for clamped–clamped isotropic circular conical shells [$r_1/h = 366$, $L/r_1 = 2.83$, $h = 0.005$ in. (0.000127 m), $\alpha = 10.4 \times 10^{-6}/^\circ\mathrm{F}$ ($18.72 \times 10^{-6}/^\circ\mathrm{C}$), $\phi = 15$ deg].

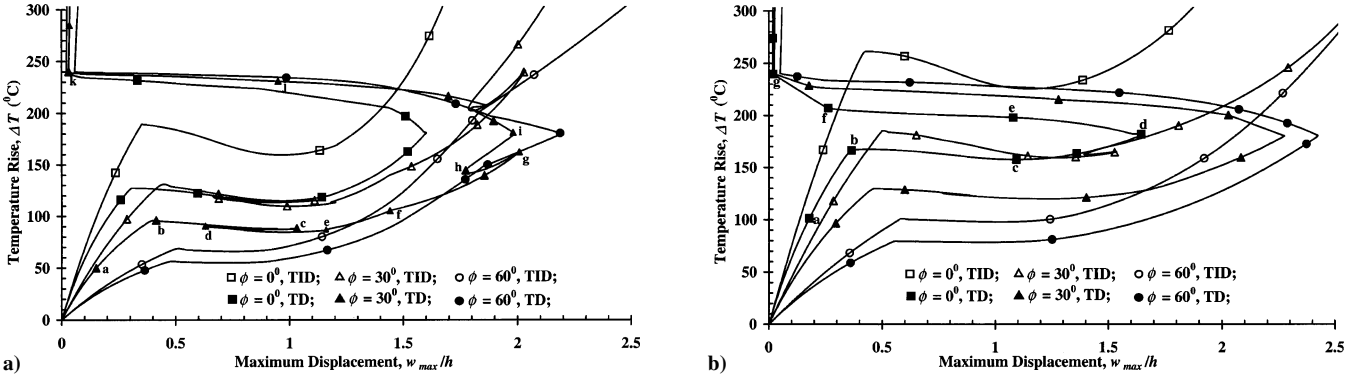

Fig. 3 Nonlinear thermoelastic response curves for cross-ply laminated simply supported conical shells ($L/r_1 = 1$, $r_1/h = 500$, material 1): a) 0/90 deg, $n = 21$; and b) $(0/90\ \text{deg})_4$, $n = 18$.

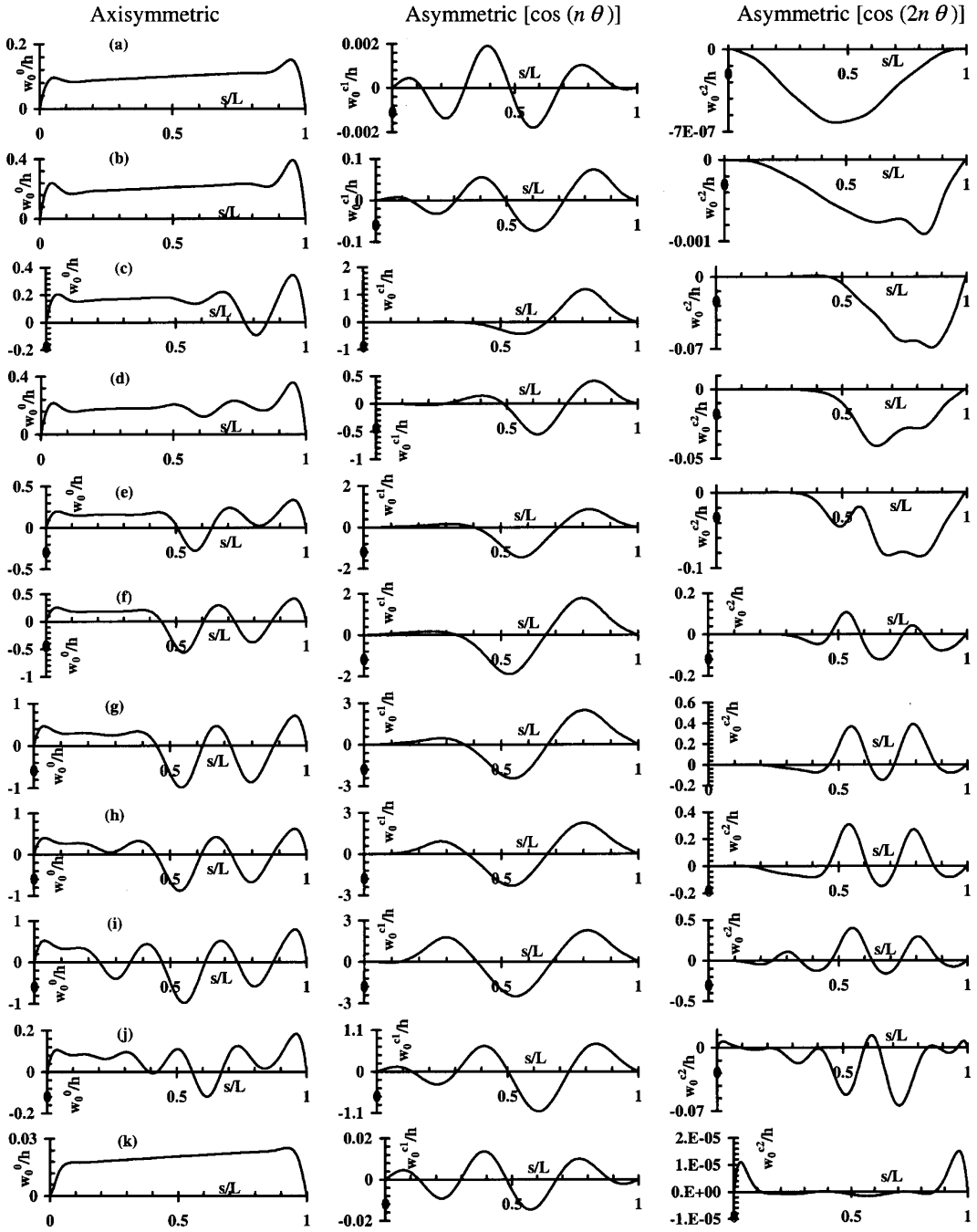

Fig. 4 Variation of normal displacement components along the meridional direction for two-layered cross-ply laminated simply supported conical shell ($L/r_1 = 1$, $r_1/h = 500$, $\phi = 30$ deg, $n = 21$).

circumferential wave numbers n chosen for the presentation of results correspond to the lowest bifurcation temperature. It is observed from this figure that the response characteristics of temperature-dependent property case are significantly different from those of temperature-independent property assumption for the geometrical and material parameters considered in this example. The equilibrium paths depicted in the figure can be divided into prebuckling range (e.g., path segment *o-a-b*), buckling/bifurcation point *b* and postbuckling range (e.g., path segment: *b-c-d-e-f-g-h-i-j-k* marked in Fig. 3a for $\phi = 30$ deg). Along the prebuckling path, the increasing trend in the rate of increase of the maximum displacement with the rise in temperature reveals the softening type of nonlinear prebuckling characteristics. It can also be noticed from Fig. 3 that the increase in the semicone angle ϕ results in a decrease in the critical bifurcation temperature and an increase in the associated prebuckling deformation level. The shells with $\phi = 0$ and 30 deg show snap-through type of postbuckling response, whereas shallow conical shells ($\phi = 60$ deg) reveal stable postbuckling behavior. The postbuckling response shows hardening type of nonlinear nature away from the vicinity of bifurcation ($w_{\max}/h \geq 1.2$). The thermal degradation of the material properties leads to the increase in the prebuckling nonlinearity and a decrease in the critical temperature and postbuckling strength. The difference in the temperature parameter corresponding to bifurcation point and minimum equilibrium temperature in the postbuckling path shows decreasing trend with the increase in the semicone angle, indicating that the sensitivity to imperfection can decrease with the increase in semicone angle. Similar interpretations have been made for panels subjected to thermomechanical loading[45] and cylindrical shells[11] exposed to temperature rise. The shell deformation in the temperature rise range (180 deg $\leq \Delta T \leq$ 240 deg) after the glass transition temperature of epoxy decreases drastically with the increase in ΔT as a result of the degradation of material properties causing the reduction in the equivalent mechanical load. For $\Delta T \geq 240$ deg, the maximum displacement again increases slowly with the rise in temperature. One can also infer from Figs. 3a and 3b that the reduction in the bending-stretching coupling caused by lamination scheme yields higher critical temperature and affects the postbuckling response noticeably.

For the purpose of analyzing the relative participation of axisymmetric w_0^0 and asymmetric w_0^{c1}, w_0^{c2} normal displacement components, their variations along the meridional direction corresponding to the points marked in Fig. 3a for conical ($\phi = 30$ deg) and in Fig. 3b for cylindrical ($\phi = 0$ deg) shells are depicted in Figs. 4 and 5, respectively. It can be inferred from Figs. 4 and 5 that the prebuckling response is dominated by axisymmetric component with significantly lower participation of asymmetric components. After the bifurcation point the postbuckling response is dominated by asymmetric components. It can further be viewed from Figs. 4 and 5 that the relative contribution and meridional variation of axisymmetric/asymmetric displacement components changes significantly after the bifurcation point. It appears that these changes in response pattern of various displacement components (w_0^0, w_0^{c1}, w_0^{c2}) leads to the decreasing trend of temperature parameter and/or maximum displacement or the formation of loops (e.g., equilibrium path segments *c-d-e* and *g-h-i* in Fig. 3a) in the postbuckling equilibrium path. Although, the unstable portion of the equilibrium path with snap-through/loops might not be realizable practically with temperature control; however, it reveals the evolution of deformation shapes after jump from one stable path portion to next one with an increase in temperature. Further, the uniform rise in temperature leads to the outward axisymmetric transverse deformation of the shell in the prebuckling range as a result of the presence of curvature causing bending-membrane coupling,[30,45] unlike the symmetrically laminated perfect flat structures where the transverse displacement is zero until the critical/bifurcation point. In the postbuckling region, the axisymmetric component has both expansion (outward) and contraction (inward) phases unlike the contraction type of nature

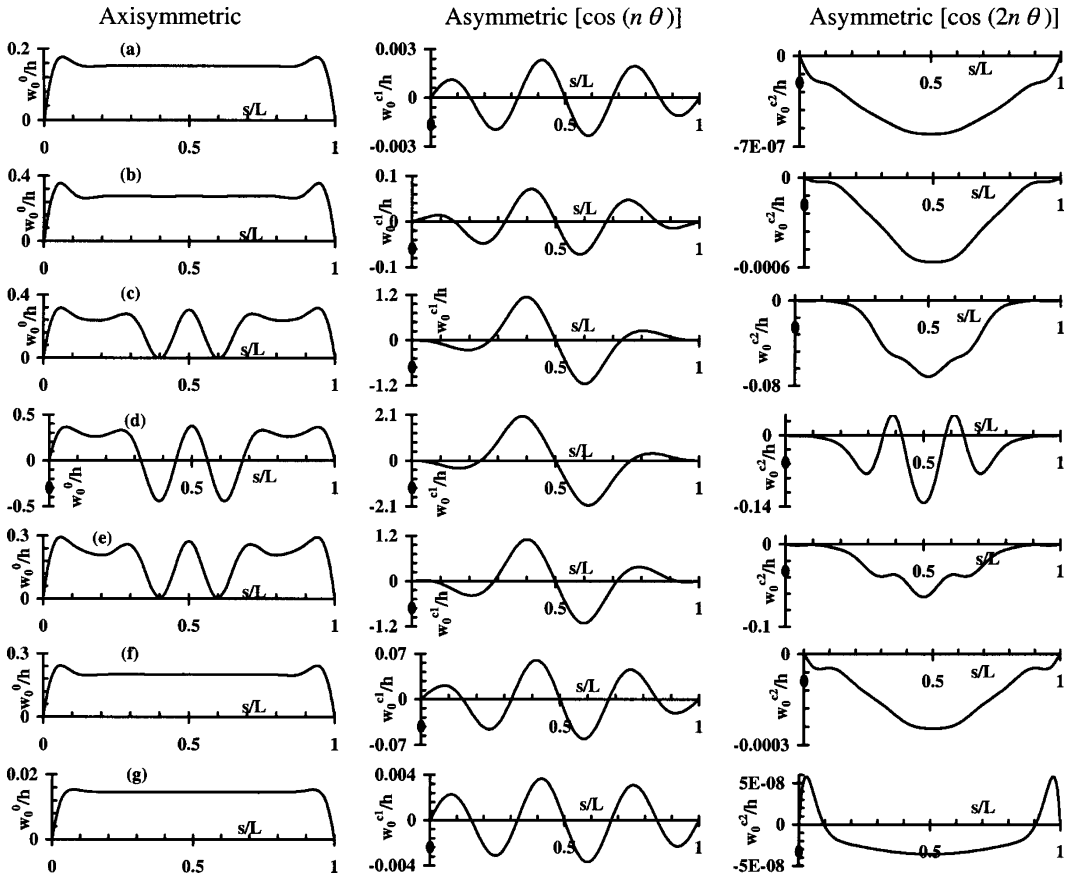

Fig. 5 Variation of normal displacement components along the meridional direction for eight-layered cross-ply laminated simply supported cylindrical shell ($L/r_1 = 1$, $r_1/h = 500$, $\phi = 0$ deg, $n = 18$).

revealed[33,35,36] in the large-amplitude asymmetric vibration of thin circumferentially closed shells. One can also infer from Fig. 4 that the stiffening effect at the smaller end of the conical shell leads to significantly lower deformation magnitude toward that end compared to the larger diameter side. However, for cylindrical shell case (see Fig. 5) the deformation pattern is symmetric/antisymmetric with respect to the center length of the shell as expected. It is also amply clear from Figs. 4 and 5 that although the participation of asymmetric mode with $2n$ circumferential waves is lower compared with axisymmetric and asymmetric mode with n circumferential waves its inclusion in the model is important for the accurate response prediction of the shells.

To study the influences of length-to-radius L/r_1 and radius-to-thickness r_1/h ratios on the nonlinear thermoelastic response behaviors, the simply supported conical shells with $(r_1/h, L/r_1) = (500, 0.5)$ and $(200, 1)$ are analyzed, and the results are depicted in Figs. 6 and 7, respectively. It can be noticed from Fig. 6 that the response characteristics of short shells ($L/r_1 = 0.5$) are, in general, qualitatively similar to those of shells with $L/r_1 = 1$. However, the critical temperature parameter and postbuckling strength are significantly higher for short shells, particularly for eight-layered case, compared with long shells considered here. Similar inferences can be drawn concerning with the influence of radius-to-thickness ratio as viewed from Fig. 7 for two-layered shells. Furthermore, the range of maximum displacement in the postbuckling region for thermal degradation cases reduces with the decrease of length-to-radius and radius-to-thickness ratios. One can also infer from Fig. 6 that the local instabilities associated with the formation of loops/turning of equilibrium path observed for shells with $L/r_1 = 1$ are absent in the characteristics of short shells studied in this example. It is also brought out in Figs. 6 and 7 that for

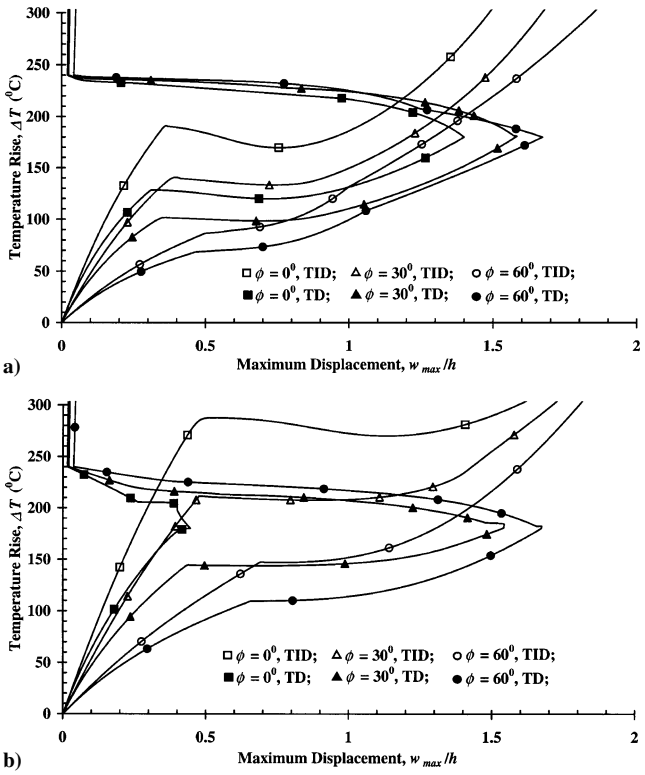

Fig. 6 Nonlinear thermoelastic response curves for cross-ply laminated simply supported conical shells ($L/r_1 = 0.5$, $r_1/h = 500$, material 1): a) 0/90 deg, $n = 21$; b) $(0/90\ \text{deg})_4$, $n = 18$.

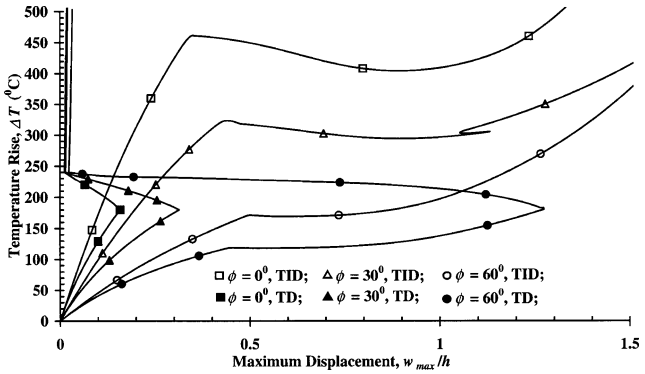

Fig. 7 Nonlinear thermoelastic response curves for cross-ply laminated simply supported conical shells ($L/r_1 = 1$, $r_1/h = 200$, material 1, 0/90 deg, $n = 13$).

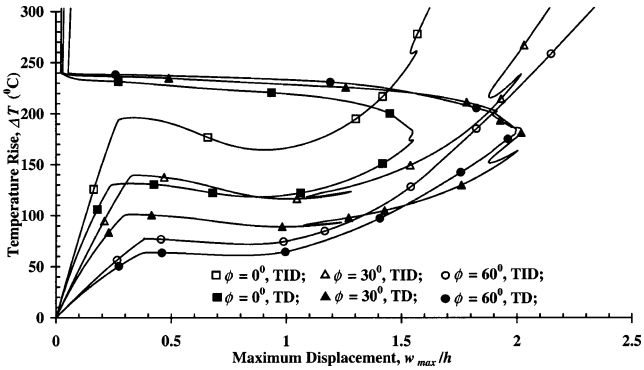

Fig. 8 Nonlinear thermoelastic response curves for cross-ply laminated clamped-clamped conical shells ($L/r_1 = 1$, $r_1/h = 500$, material 1, 0/90 deg, $n = 21$).

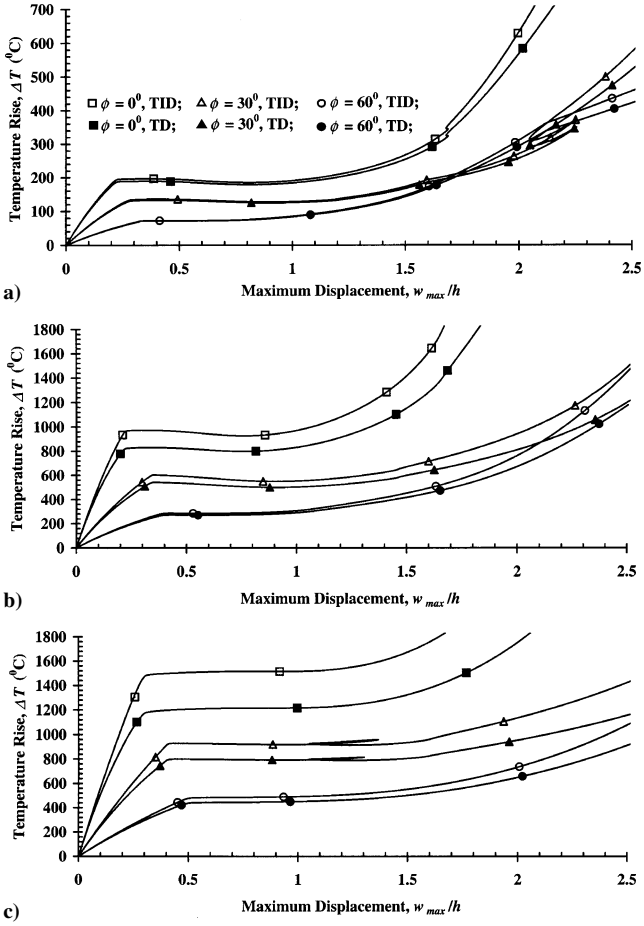

Fig. 9 Nonlinear thermoelastic response curves for cross-ply laminated simply supported conical shells (material 2): a) $L/r_1 = 1$, $r_1/h = 500$, 0/90 deg, $n = 20$; b) $L/r_1 = 2$, $r_1/h = 100$, 0/90 deg, $n = 9$; and c) $L/r_1 = 2$, $r_1/h = 100$, $(0/90\ \text{deg})_4$, $n = 8$.

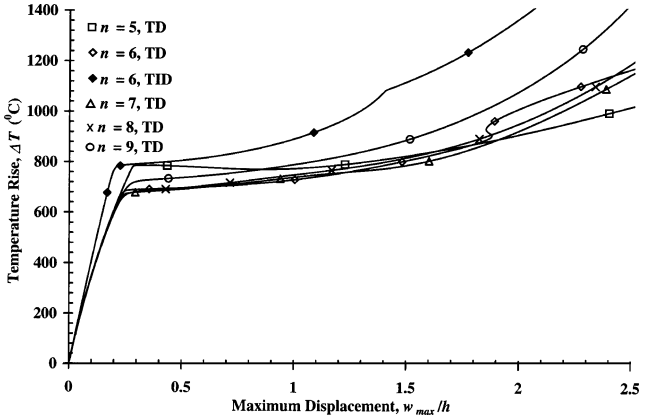

Fig. 10 Nonlinear thermoelastic response curves for cross-ply laminated simply supported conical shell ($L/r_1 = 2$, $r_1/h = 100$, $(0/90\ \text{deg})_{2S}$, $\phi = 30$ deg, material 3).

certain shell parameters [$(r_1/h = 500, L/r_1 = 0.5, \phi = 0$ deg) and $(r_1/h = 200, L/r_1 = 1, \phi = 0$ and 30 deg)] with thermal degradation of material properties the asymmetric bifurcation buckling/postbuckling response behavior might not be realized.

To highlight the sensitivity of thermoelastic response behavior of shells to boundary conditions, the analysis is also carried out for clamped-clamped immovable support conditions, and the results for one case ($L/r_1 = 1, r_1/h = 500$, 0/90 deg, material 1) are highlighted in Fig. 8. It can be concluded from the comparison of Figs. 8 and 3 that the sensitivity of thermoelastic response characteristics to the rotational edge restraints is very less for the shells considered here. It might slightly influence the extent of local instabilities such as formation of loops/turning of equilibrium path as seen in Fig. 8.

Finally, the pre- and postbuckling characteristics of simply supported shells made up of material 2 and material 3 are analyzed, and the results are shown in Figs. 9 and 10. It is observed from these figures that the prebuckling thermoelastic response behavior is qualitatively similar to that of shells of material 1. However, the postbuckling response, which is of stable nature, is significantly different particularly for shells with thermal degradation of properties. It can be seen from these figures that the difference in the thermoelastic response characteristics of shells with and without thermal degradation of properties is dominant only at higher temperature ranges. Therefore, for the shell parameters yielding lower bifurcation/buckling temperature, the incorporation of thermal degradation of properties for the response predication might not be essential. The influence of circumferential wave number n highlighted in Fig. 10 reveals that postbuckling characteristics pertaining to wave numbers close to the critical wave number n_{cr} corresponding to lowest bifurcation temperature differ slightly at lower displacement magnitude. However, the wave numbers resulting in higher bifurcation temperature can yield lower postbuckling temperature at higher displacement magnitudes. It can therefore be concluded that the wave number corresponding to lowest temperature can change with the postbuckling response amplitude.

V. Conclusions

The nonlinear thermoelastic buckling/postbuckling characteristics of laminated circular conical/cylindrical shells subjected to uniform temperature rise are studied employing semi-analytical finite element approach. The influence of thermal degradation of material properties is highlighted considering different material/geometrical parameters. The participation of axisymmetric and asymmetric modes in the total response of the shells is brought out through the deformation shape analysis. The following observations can be made from the detailed analysis carried out here:

1) The thermal degradation of material properties can significantly affect the thermoelastic response characteristics depending on the geometrical and material parameters.

2) The prebuckling responses of the shells reveal softening type of nonlinear nature.

3) The increase in the semicone angle results in a decrease in the critical bifurcation temperature, an increase in the associated prebuckling deformation level, and a decrease in the sensitivity to imperfections.

4) The postbuckling response shows a hardening type of nonlinear nature away from the vicinity of bifurcation.

5) The thermal degradation of the material properties leads to the increase in the prebuckling nonlinearity and a decrease in the critical temperature and postbuckling strength.

6) The axisymmetric transverse deformation of the shell in the prebuckling range is outward, whereas in the postbuckling region it has both expansion (outward) and contraction (inward) phases unlike the contraction type of nature in the large-amplitude asymmetric vibration of shells.

7) The stiffening effect toward the smaller diameter edge of the conical shell leads to significantly lower deformation magnitude towards that end compared to the larger diameter side, whereas the deformation pattern is symmetric/antisymmetric with respect to the center length for the cylindrical shells.

8) The participation of asymmetric mode with $2n$ circumferential waves is lower compared to axisymmetric and asymmetric mode with n circumferential waves, but its inclusion in the model is important for the accurate response prediction of the shells.

9) The sensitivity of thermoelastic response characteristics to the rotational edge restraints is found to be very less for the geometrical parameters assumed here.

10) The circumferential wave number corresponding to lowest temperature can change with the postbuckling response amplitude of the shells.

References

[1]Thornton, E. A., "Thermal Buckling of Plates and Shells," *Applied Mechanics Reviews*, Vol. 46, No. 10, 1993, pp. 485–506.

[2]Noor, A. K., and Burton, W. S., "Computational Models for High-Temperature Multilayered Composite Plates and Shells," *Applied Mechanics Reviews*, Vol. 45, No. 10, 1992, pp. 419–446.

[3]Argyris, J. H., and Tenek, L., "Recent Advances in Computational Thermostructural Analysis of Composite Plates and Shells with Strong Nonlinearities," *Applied Mechanics Reviews*, Vol. 50, No. 5, 1997, pp. 285–305.

[4]Thangartnam, R. K., Palaninathan, R., and Ramachandran, J., "Buckling of Composite Cylindrical Shells," *Journal of the Aeronautical Society of India*, Vol. 41, No. 1, 1989, pp. 47–54.

[5]Thangartnam, R. K., Palaninathan, R., and Ramachandran, J., "Thermal Buckling of Lamianted Composite Shells," *AIAA Journal*, Vol. 28, No. 5, 1990, pp. 859–860.

[6]Eslami, M. R., and Javaheri, M. R., "Thermal and Mechanical Buckling of Composite Cylindrical Shells," *Journal of Thermal Stresses*, Vol. 22, No. 6, 1999, pp. 527–545.

[7]Ganesan, N., and Kadoli, R., "Buckling and Dynamic Analysis of Piezothermoelastic Composite Cylindrical Shells," *Composite Structures*, Vol. 59, No. 1, 2003, pp. 45–60.

[8]Kadoli, R., and Ganesan, N., "Free Vibration and Buckling Analysis of Composite Cylindrical Shells Conveying Hot Fluid," *Composite Structures*, Vol. 60, No. 1, 2003, pp. 19–32.

[9]Birman, V., and Bert, C. W., "Buckling and Post-Buckling of Composite Plates and Shells Subjected to Elevated Temperature," *Journal of Applied Mechanics*, Vol. 60, June 1993, pp. 514–519.

[10]Shen, H.-S., "Thermomechanical Postbuckling Analysis of Stiffned Laminated Cylindrical Shell," *Journal of Engineering Mechanics*, Vol. 123, No. 5, 1997, pp. 433–443.

[11]Shen, H.-S., "Thermal Postbuckling Analysis of Imperfect Stiffened Laminated Cylindrical Shells," *International Journal of Nonlinear Mechanics*, Vol. 32, No. 2, 1997, pp. 259–275.

[12]Shen, H.-S., "Postbuckling Analysis of Imperfect Stiffened Laminated Cylindrical Shells Under Combined External Pressure and Thermal Loading," *International Journal of Mechanical Sciences*, Vol. 40, No. 4, 1998, pp. 339–355.

[13]Shen, H.-S., "Postbuckling of Laminated Cylindrical Shells with Piezoelectric Actuators Under Combined External Pressure and Heating," *International Journal of Solids and Structures*, Vol. 39, No. 16, 2002, pp. 4271–4289.

[14]Shen, H.-S., "Thermomechanical Postbuckling of Shear Deformable Laminated Cylindrical Shells with Local Geometric Imperfections," *International Journal of Solids and Structures*, Vol. 39, No. 17, 2002, pp. 4525–4542.

[15]Birman, V., "Thermal Dynamic Problems of Reinforced Composite Cylinders," *Journal of Applied Mechanics*, Vol. 57, Dec. 1990, pp. 941–947.

[16]Shariyat, M., and Eslami, M. R., "Dynamic Buckling and Postbuckling of Imperfect Orthotropic Cylindrical Shells Under Mechanical and Thermal Loads, Based on the Three-Dimensional Theory of Elasticity," *Journal of Applied Mechanics*, Vol. 66, June 1999, pp. 476–484.

[17]Birman, V., and Bert, C. W., "Dynamic Stability of Reinforced Composite Cylindrical Shells in Thermal Fields," *Journal of Sound and Vibration*, Vol. 142, No. 2, 1990, pp. 183–190.

[18]Bendavid, D., and Singer, J., "Buckling of Conical Shells Heated Along a Generator," *AIAA Journal*, Vol. 5, No. 9, 1967, pp. 1710–1713.

[19]Lu, S. Y., and Chang, L. K., "Thermal Buckling of Conical Shells," *AIAA Journal*, Vol. 5, No. 10, 1967, pp. 1877–1882.

[20]Chang, L. K., and Lu, S. Y., "Nonlinear Thermal Elastic Buckling of Conical Shells," *Nuclear Engineering and Design*, Vol. 7, No. 2, 1968, pp. 159–169.

[21]Tani, J., "Influence of Axisymmetric Initial Deflections on the Thermal Buckling of Truncated Conical Shells," *Nuclear Engineering and Design*, Vol. 48, No. 2–3, 1978, pp. 393–403.

[22]Tani, J., "Buckling of Truncated Conical Shells Under Combined Pressure and Heating," *Journal of Thermal Stresses*, Vol. 7, 1984, pp. 307–316.

[23]Wu, C.-P., and Chiu, S.-J., "Thermoelastic Buckling of Laminated Composite Conical Shells," *Journal of Thermal Stresses*, Vol. 24, No. 9, 2001, pp. 881–901.

[24]Wu, C.-P., and Chiu, S.-J., "Thermally Induced Dynamic Instability of Laminated Composite Conical Shells," *International Journal of Solids and Structures*, Vol. 39, No. 11, 2002, pp. 3001–3021.

[25]Hoff, N. J., "Buckling at High Temperature," *Journal of Royal Aeronautical Society*, Vol. 61, 1957, pp. 756–774.

[26]Chen, L.-W., and Chen, L.-Y., "Thermal Postbuckling Behaviors of Laminated Composite Plates with Temperature-Dependent Properties," *Composite Structures*, Vol. 19, No. 3, 1991, pp. 267–283.

[27]Singha, M. K., Ramachandra, L. S., and Bandyopadhyay, J. N., "Thermal Postbuckling Analysis of Laminated Composite Plates," *Composite Structures*, Vol. 54, No. 4, 2001, pp. 453–458.

[28]Srikanth, G., and Kumar, A., "Postbuckling Response and Failure of Symmetric Laminates Under Uniform Temperature Rise," *Composite Structures*, Vol. 59, No. 1, 2003, pp. 109–118.

[29]Shukla, K. K., Huang, J. H., and Nath, Y., "Thermal Postbuckling of Laminated Composite Plates with Temperature Dependent Properties," *Journal of Engineering Mechanics*, Vol. 130, No. 7, 2004, pp. 818–825.

[30]Singha, M. K., Ramachandra, L. S., and Bandyopadhyay, J. N., "Thermomechanical Postbuckling Responses and First-Ply Failure Analysis of Doubly Curved Panels," *AIAA Journal*, Vol. 41, No. 10, 2003, pp. 2486–2491.

[31]Wang, X., Lu, G., and Xiao, D. G., "Non-Linear Thermal Buckling for Local Delamination near the Surface of Laminated Cylindrical Shell," *International Journal of Mechanical Sciences*, Vol. 44, No. 5, 2002, pp. 947–965.

[32]Ganapathi, M., Gupta, S. S., and Patel, B. P., "Nonlinear Asymmetric Dynamic Buckling of Isotropic/Laminated Orthotropic Spherical Caps," *AIAA Journal*, Vol. 41, No. 7, 2003, pp. 1363–1369.

[33]Ueda, T., "Nonlinear Free Vibrations of Conical Shells," *Journal of Sound and Vibration*, Vol. 64, No. 1, 1979, pp. 85–95.

[34]Tong, P., and Pian, T. H. H., "Postbuckling Analysis of Shells of Revolution by the Finite Element Method," *Thin Shell Structures*, edited by Y. C. Fung and E. E. Sechler, Prentice–Hall, Upper Saddle River, NJ, 1974, pp. 435–452.

[35]Amabili, M., Pellicano, F., and Paidoussis, M. P., "Non-Linear Dynamics and Stability of Circular Cylindrical Shells Containing Flowing Fluid, Part II: Large Amplitude Vibrations Without Flow," *Journal of Sound and Vibration*, Vol. 228, No. 5, 1999, pp. 1103–1124.

[36]Patel, B. P., Ganapathi, M., Makhecha, D. P., and Shah, P., "Large Amplitude Free Flexural Vibration of Rings Using Finite Element Approach," *International Journal of Non-Linear Mechanics*, Vol. 37, No. 6, 2003, pp. 911–921.

[37]Kraus, H., *Thin Elastic Shells*, Wiley, New York, 1976.

[38]Jones, R. M., *Mechanics of Composite Materials*, McGraw–Hill, New York, 1975.

[39]Rajasekaran, S., and Murray, D. W., "Incremental Finite Element Matrices," *Journal of the Structural Division*, Vol. 99, No. ST12, 1973, pp. 2423–2438.

[40]Batoz, J. L., and Dhatt, G., "Incremental Displacement in Nonlinear Analysis," *International Journal for Numerical Methods in Engineering*, Vol. 14, No. 8, 1979, pp. 1262–1267.

[41]Bergan, P. G., and Clough, R. W., "Convergence Criteria for Iterative Process," *AIAA Journal*, Vol. 10, No. 8, 1972, pp. 1107,1108.

[42]Balakrishna, C., and Sarma, B. S., "Analysis of Axisymmetric Shells Subjected to Asymmetric Loads Using Field Consistent Shear Flexible Curved Element," *Journal of the Aeronautical Society of India*, Vol. 41, No. 1, 1989, pp. 89–95.

[43]Prathap, G., and Ramesh Babu, C., "A Field-Consistent Three-Noded Quadratic Curved Axisymmetric Shell Element," *International Journal for Numerical Methods in Engineering*, Vol. 23, No. 4, 1986, pp. 711–723.

[44]Chen, J. K., Sun, C. T., and Chang, C. I., "Failure Analysis of a Graphite/Epoxy Laminate Subjected to Combined Thermal and Mechanical Loading," *Journal of Composite Materials*, Vol. 19, No. 5, 1985, pp. 408–423.

[45]Librescu, L., Nemeth, M. P., Starnes, J. H., and Lin, W., "Nonlinear Response of Flat and Curved Panels to Thermomechanical Loading," *Journal of Thermal Stresses*, Vol. 23, No. 6, 2000, pp. 549–582.

B. Sankar
Associate Editor